DePaul University
UNIVERSITY LIBRARIES

DePaul Discoveries

Volume 10 | Issue 1 Article 16

2021

Triangulation and finite element method for a variational problem inspired by medical imaging

Tim Komperda
DePaul University, tkomperd@depaul.edu

Enrico Au-Yeung
DePaul University, eauyeun1@depaul.edu

Recommended Citation

Komperda, Tim and Au-Yeung, Enrico (2021) "Triangulation and finite element method for a variational problem inspired by medical imaging," *DePaul Discoveries*: Vol. 10 : Iss. 1 , Article 16.
Available at: https://via.library.depaul.edu/depaul-disc/vol10/iss1/16

Triangulation and finite element method for a variational problem inspired by medical imaging

Acknowledgements

The first author is grateful for the financial support of an Undergraduate Summer Research Program (USRP) grant from DePaul University. The second author is grateful that the Undergraduate Summer Research Program (USRP) grant from DePaul University makes this research project possible.

Triangulation and finite element method for a variational problem inspired by medical imaging

Tim Komperda*

Department of Mathematical Sciences

Enrico Au-Yeung, PhD

Department of Mathematical Sciences

ABSTRACT We implement the finite element method to solve a variational problem that is inspired by medical imaging. In our application, the domain of the image does not need to be a rectangle and can contain a cavity in the middle. The standard approach to solve a variational problem involves formulating the problem as a partial differential equation. Instead, we solve the variational problem directly, using only techniques available to anyone familiar with vector calculus. As part of the computation, we also explore how triangulation is a useful tool in the process.

INTRODUCTION

Breast cancer has caused a lot of distress, both to the people with it and the family of the patient. Some of this distress can be alleviated if the disease is caught in the early stages. Thus, cancer screenings are insurmountably valuable. One such screening used is the mammogram to detect breast cancer. Mammograms have an inconclusive rate of at least 10 percent (see [1]). With approximately 60 percent of the 150 million women in the United States receiving mammograms (see [6]) in the last two years, this means that the 10 percent of inconclusive mammograms affected approximately 9 million women. The problem we solve in this project is inspired by the need to tackle inconclusive results like these by improving the quality of the images around possible tumor areas.

Improving the quality in a particular area of the image can be formulated as a variational problem. Typically, issues like this in image processing are solved by using a rectangular table of entries called pixels. These pixels would have values ranging from 0 representing the color black to 255 representing white. However, in medical imaging the domain of the image is not guaranteed to be a rectangle therefore causing issues when trying to apply the standard methods. In this paper, we propose that using the Finite Element Method (FEM) and different methods of triangulations; we minimize the Dirichlet integral to find the smoothest function that agrees with the higher-quality data on the boundary of the domain. This smoothest function will give radiologists an idea of how the area inside the boundary would look. We are particularly

* *tkomperd@depaul.edu*

Research completed in Winter 2021

interested in a triangle with a circular hole as the domain, or any polygon with an internal cavity. These are shapes that represent a collection of tissue cells which may be blurry and causing a radiologist to call a test inconclusive.

The result from the mammogram is inconclusive if the image taken is blurry. The quality of data over the boundaries is high, but the quality of data is low in the interior.

If we regard the pixels of the image as a function $u(x, y)$, where the point (x, y) is the location of the pixel, we can also treat $u(x, y)$ as a surface over a domain. Using only the clean data from the boundary, we want to find the smoothest surface with the given boundary condition. This motivates the need to solve for a function u(x, y) as a variational problem. The standard approach to solve a variational problem involves formulating the problem as a partial differential equation. Instead, we solve the variational problem by a direct method.

As part of the computation, we also explore how triangulation is a useful tool in the process.

Solving the problem by the Finite Element Method

Let D be a bounded domain in the plane with a piecewise smooth boundary. A domain is any connected open set, which we can think of as any polygon and it may have a hole inside. Given a function $z(x, y)$, we want to find the smoothest surface u(x, y) that agrees with the given function on the boundary.

To formulate this problem, we want to find a function $u(x, y)$ that minimizes the Dirichlet integral,

$$I = \iint_D \left\{ \left(\frac{\partial u}{\partial x}\right)^2 + \left(\frac{\partial u}{\partial y}\right)^2 \right\} dA \qquad (1)$$

subject to the condition: $u(x, y) = z(x, y)$ on the boundary of D. The integrand is the square of the length of the gradient vector of $u(x, y)$. The integral measures the smoothness of a surface. If we do not impose the boundary condition, the problem becomes uninteresting; we can set the function $u(x, y)$ to be zero. The integral depends on the function $u(x, y)$, which takes an input u and computes a number as the output. As the input function u(x, y) varies, the output number will vary. To avoid taking square root, we minimize the square of the length of the gradient vector. This problem of minimizing the Dirichlet integral is an example of a variational problem.

We use the finite element method to minimize the Dirichlet integral. We divide the domain D into p triangles $\{T_i\}_{i=1}^{p}$. Instead of considering the set of all continuous functions, we consider a special class of continuous functions. Let $u(x, y)$ be a linear combination of local basis functions,

$$u(x, y) = \sum_{j=1}^{n} c_j \phi_j(x, y) \qquad (2)$$

where each $\phi_j(x, y)$ is a linear function on each triangle. Here, n is the total number of vertices of all triangles. In specifying $u(x, y)$, the constants c_j are the unknown variables.

The local basis functions $\phi_j(x, y)$ are determined by the triangles. We choose the constants c_j to minimize the Dirichlet integral, while satisfying the boundary condition. The mathematical details are provided in the Appendix.

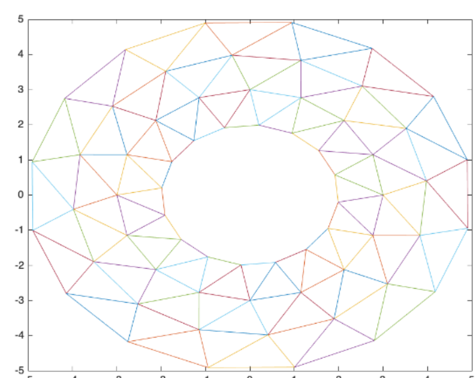

Figure 1. Triangulation of a domain

The basis functions ϕ_j(x, y) depend on the triangles. We need a way to divide the domain into many triangles. The edges of the triangles do not cross each other. As an illustration, consider a ring-shaped domain, also known as an annulus. Figure 1 shows the division of this domain into many triangles. Triangulation is any method that makes a division of a domain into non-crossing triangles. The domain can be any polygon and it can contain a hole inside. One way to construct a triangulation of a shape is to exploit its connection to a Voronoi diagram.

Triangulation and Voronoi diagram

In the context of Voronoi diagrams, the points of a finite set S are often called sites. Imagine that each site in S represents a post office. If your home is in the plane, then naturally you want to go to the post office closest to your house. If p is the location of a post office, you can also consider the region of points that are each closer to p than to any other site in S. The division of the plane into these regions is called the Voronoi diagram of the point set, with each region a Voronoi region. Figure 2 shows the Voronoi diagram for seven post offices.

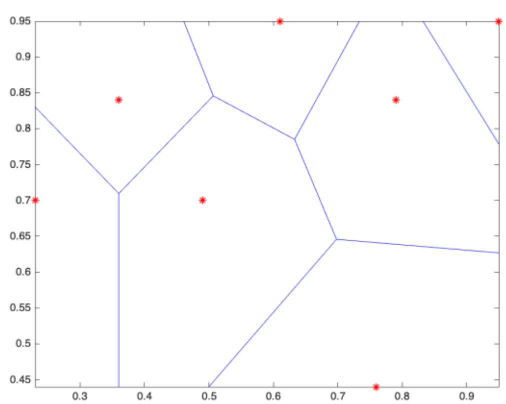

Figure 2. The Voronoi diagram for 7 sites

Let S be a collection of sites in the plane. The Voronoi region of a site p in S is

$$\mathrm{Vor}(p) = \{x \in \mathrm{R}^2 : ||x - p|| \leq ||x - q||\} \text{ for all sites q in S,}$$

Where $||p - q||$ denotes the Euclidean distance between points p and q in the plane. In words, $\mathrm{Vor}(p)$ is the set of all the points in the plane that are at least as close to p than to any other site q in S. There are points that lie on the

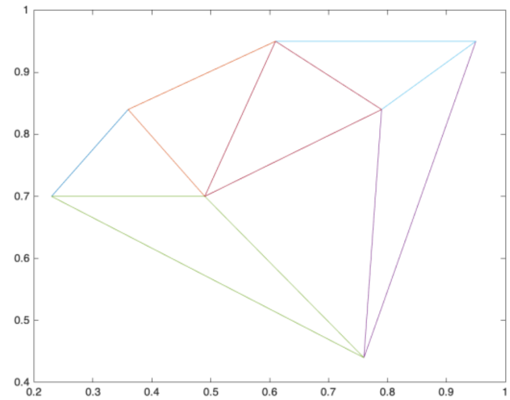

Figure 3. The straight-line dual graph of the Voronoi diagram

A fundamental result in computational geometry is that Delaunay triangulation is the dual of the Voronoi diagram. The vertices of the dual graph are the sites of the point set S, and two sites are connected by a straight line if they share a common boundary. Figure 3 shows the Delaunay triangulation for seven post offices, obtained as the dual graph of the Voronoi diagram in figure 2

For a lucid discussion on Voronoi diagram and Delaunay triangulation, we refer the interested reader to [5]. There are many triangulations for a domain. When we first did this project, before we used Delaunay triangulation, we explored with our own method of triangulation; we call it Atlantis triangulation. The division of the annulus into 96 triangles illustrated in figure 1 is an example of Atlantis triangulation. We provide a brief explanation of this procedure in the Appendix.

Related Works

It might appear more natural to use the length of the gradient vector instead of its square. Let ∇u be the gradient vector. Minimizing the length of ∇u is not a smooth optimization problem. That is a far more challenging problem beyond the scope of our project. The non-smooth eigenvalue problem is to solve for a function $u(x, y)$ to minimize $\int_D |\nabla u(x, y)|^2 \, dA$, subject to the constraint that $\int_D |u(x, y)|^2 \, dA = 1$.

The finite element method is used in [3] to solve this problem. The authors find that whether the finite element solution converges to the true global minimum can depend on the geometry of the domain.

Variational problems in image processing have been investigated by many researchers. See, for example, [2], [4], [7], [8]. In these works, the task is to remove noise from an image or to restore a blurry image. The domain of the image is a rectangle.

Numerical Experiments

We illustrate our method with two examples. Given a function $z(x, y)$, we solve for a function $u(x, y)$ that agrees with $z(x, y)$ on the outer boundary and the inner boundary.

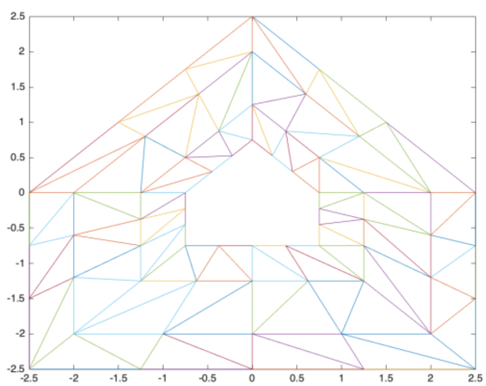

Figure 4. Atlantis triangulation of the shape from Example 1

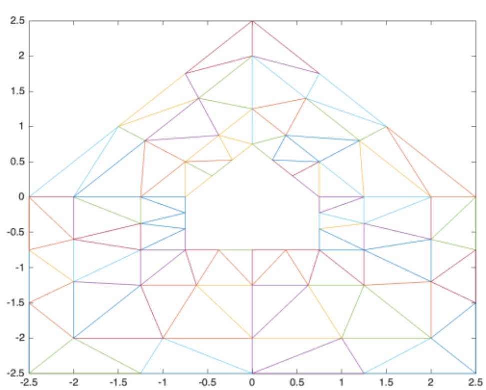

Figure 5. Delaunay triangulation of the shape from Example 1

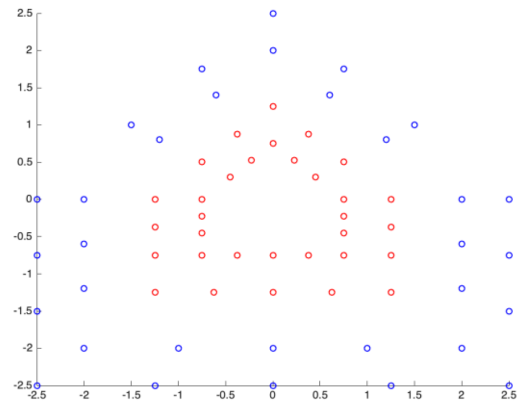

Figure 6. Vertices of the triangles in the shape from Example 1

Example 1

Suppose the shape D is a pentagon with a pentagon cavity. The boundary of D consists of two pieces: the outer boundary of the pentagon and the inner boundary of the cavity in the middle. Figure 4 shows the triangulation of the shape. Figure 5 shows the Delaunay triangulation of the shape. To make the triangulation, we need to first specify the vertices of the triangles. Figure 6 shows the triangulation of the shape. Suppose $z(x, y) = x + y + 5$. This is a plane. The finite element solution $u(x, y)$ constructed using either Delaunay or Atlantis triangulation completely reconstructs $z(x, y)$ on the interior of the domain. Figure 7 shows the initial surface given by $u(x, y) = x + y + 5$ when (x, y) is on the outer boundary and inner boundary, and $u(x, y) = 0$ when (x, y) is on the interior of the domain. Figure 8 shows the surface $u(x, y)$ constructed by using finite element method. To make the example more interesting, suppose $z(x, y) = x^2 - y^2$. This surface is a horse saddle. Now, $u(x, y)$ is the smoothest surface that must agree with $z(x, y)$ on the outer boundary and the inner boundary. In this sense, among all piecewise-linear functions, $u(x, y)$ is the best approximation of the saddle. How accurate is this approximation on the interior?

Among the 64 vertices shown in Figure 6, there are 16 vertices on the outer boundary (blue points on outer pentagon) and 16 vertices on the inner boundary (red points on a smaller pentagon in the middle). By construction, $\mathrm{u}(x, y) = \mathrm{z}(x, y)$ on these 32 vertices. In the remaining 32 vertices on the interior of the domain, we can calculate the error ϵ,

$$\epsilon = \frac{||u - z||}{||z||} \qquad (3)$$

where, the norm $|| \cdot ||$ is the Euclidean norm, i.e. $||u - z||^2 = \sum_{j=1}^{32} \big(u(j) - z(j)\big)^2$ Here, by a slight abuse of notation, the variables $u(j)$ and $z(j)$ are, respectively, the values of u and z on the 32 internal vertices. The sum is from $j = 1$ to $j = 32$ because we are adding over all the internal vertices.

Figure 9 shows the initial surface given by $\mathrm{u}(x, y) = x^2 - y^2$ when (x, y) is on the outer boundary and inner boundary, and $\mathrm{u}(x, y) = 0$ when (x, y) is on the interior of the domain. Figure 10 shows the surface $\mathrm{u}(x, y)$for the saddle constructed by using finite element method. The computation using finite element method (with Delaunay triangulation) shows that $\mathrm{u}(x, y)$ does a reasonably well to approximate $\mathrm{z}(x, y)$ on the interior of the surface; the error is 0.95 percent. For a quick comparison, on four of the inner vertices, the values of u are

$$[0.3186, -0.6727, -1.5985, -0.6727]$$

and the corresponding values of z are

$$[0.3125, -0.6250, -1.5625, -0.6250].$$

The finite element solution with Atlantis triangulation shows a comparable result.

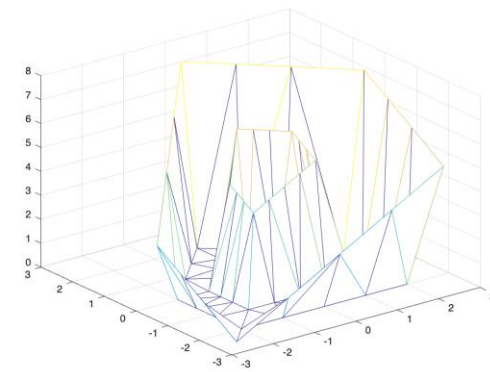

Figure 7. The initial surface $u(x,\ y)$from Example 1

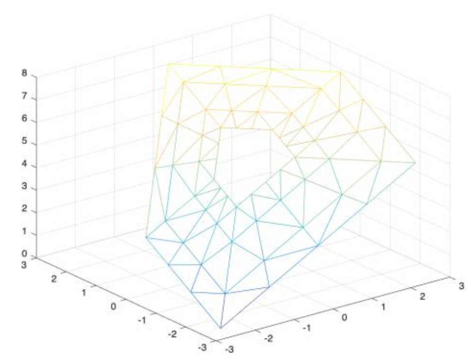

Figure 8. The solution of $u(x,\ y)$ for the plane from Example 1

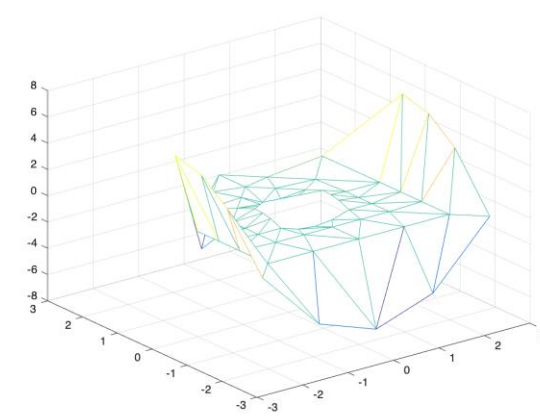

Figure 9. The initial surface $u(x,\ y)$ of saddle from Example 1

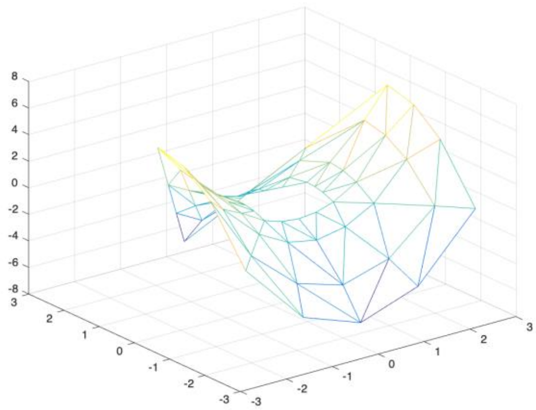

Figure 10. The solution of $u(x, y)$ for the saddle $x^2 - y^2$ from Example 1

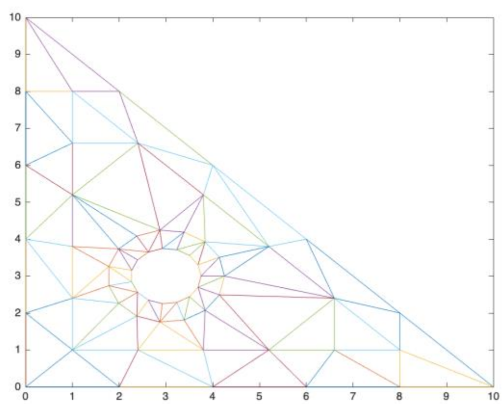

Figure 11. Delaunay triangulation of the shape from Example 2

Example 2

Suppose the shape D is a triangle with a circular cavity. The boundary of D consists of two pieces: the outer boundary is a triangle, and the inner boundary is a circle in the middle. Figure 11 shows the triangulation of the shape. Suppose $z(x, y) = x + y + 5$. This a plane, and since $u(x, y)$ is the best linear function that agrees with $z(x, y)$ on the boundary, $u(x, y)$ is exactly equal to $z(x, y)$ in this case, as to be expected.

Following Example 1, we next consider $z(x, y) = x^2 - y^2$, the horse saddle. The computation using finite element method shows that $u(x, y)$ does a reasonably well to approximate $z(x, y)$on the interior of the surface; the error is 0.54 percent. For a quick comparison, on five of the inner vertices, the values of u are

$$[4.7902, 13.4896, 26.6379, 42.7864, 62.8647]$$

and the corresponding values of z are

$$[4.76,\ 13.44,\ 26.04,\ 42.56,\ 63.00].$$

Figure 12 shows the initial surface given by $u(x, y) = x^2 - y^2$when (x, y) is on the outer boundary and inner boundary, and $u(x, y) = 0$ when (x, y) is on the interior of the domain. Figure 13 shows the surface $u(x, y)$ constructed by using finite element method.

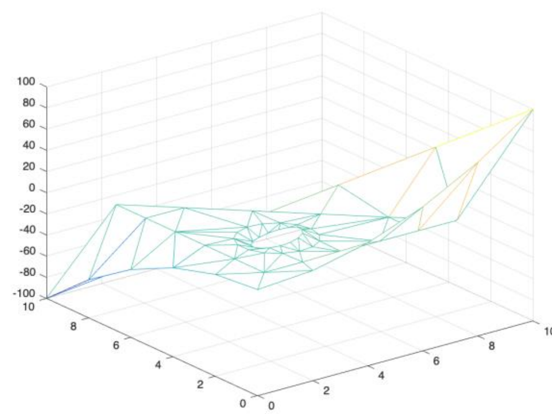

Figure 12. The initial surface $u(x, y)$ for the saddle from Example 2

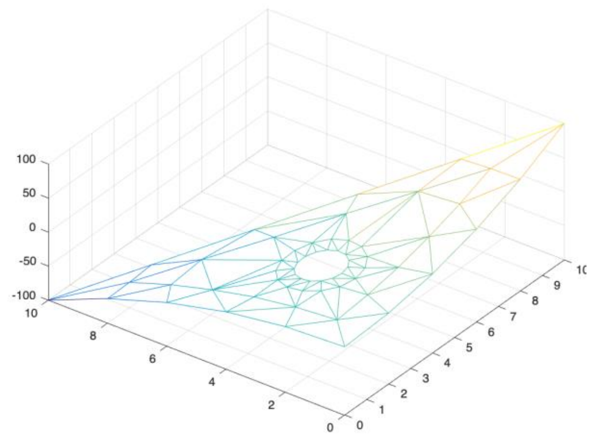

Figure 13. The solution of $u(x, y)$ for the saddle from Example 2

Conclusion

We implement the finite element method to solve a variational problem that is inspired by medical imaging using only techniques available to anyone familiar with vector calculus. The domain of the image does not need to be a rectangle and can contain a cavity in the middle.

The standard approach to solve a variational problem involves formulating the problem as a partial differential equation. Instead, we solve the variational problem by a direct method. As part of the computation, we also explore how triangulation is a useful tool in the process. We suspect that when the number of vertices is large, dividing a domain into triangles with Atlantis triangulation can be much faster than Delaunay triangulation. We leave the exploration of triangulation and more examples to future research.

ACKNOWLEDGEMENTS

The first author is grateful for the financial support of an Undergraduate Summer Research Program (USRP) grant from DePaul University.

The second author is grateful that the Undergraduate Summer Research Program (USRP) grant from DePaul University makes this research project possible.

REFERENCES

[1] Breast Cancer Surveillance Consortium (BCSC). Sensitivity, specificity, and false negative rate for 1,682,504 screening mammography examinations from 2007-2013. https://www.bcsc-research.org/statistics/screening-performance-benchmarks/screening-sens-spec-false-negative, 2017.

[2] Burger, M., Gilboa, G., Osher, S., and Xu, J. (2006). *Nonlinear inverse scale space methods, Communications in Mathematical Sciences*, 4, no. 1, 179–212.

[3] Caboussat, A., Glowinski, R., and Pons, V. (2009). *An Augmented Lagrangian Approach to the Numerical Solution of a Non-Smooth Eigenvalue Problem*, Numer, J. Math. , 17, no. 7, 3–26.

[4] Chan, T. F., Golub, G. H., and Mulet, P. (1999). *A nonlinear primal-dual method for total variation-based image restoration, SIAM Journal on Scientific Computing*, 20, no. 6, 1964–1977.

[5] Devadoss, S. and O'Rourke, J. (2011). *Discrete and Computational Geometry*, Princeton University Press, 255 pages.

[6] *Final Recommendation Statement: Breast Cancer: Screening*, US Preventive Services Task Force. January 2016.

[7] Kärkkäinen, T., Kunisch, K., and Majava, K. (2005). *Denoising of smooth images using L 1-fitting*, *Computing*, 74, no. 4, 353–376.

[8] Sciacchitano, F., Dong, Y., Jain, P., and Zeng, T. (2015). *Variational approach for restoring blurred images with Cauchy noise,* SIAM Journal on Imaging Sciences, 8, no. 3, 1894–1922.

APPENDIX

We provide the detail of how we use the finite element method for the variational problem. We also briefly describe how to partition a domain into triangles using Atlantis triangulation.

Applying the Finite Element Method

We are given a function $z(x, y)$. The problem is to minimize the Dirichlet integral,

$$I = \iint_D \left[\left(\frac{\partial u}{\partial x}\right)^2 + \left(\frac{\partial u}{\partial y}\right)^2 \right] dA \tag{4}$$

with the condition: $u(x, y) = z(x, y)$ on the boundary of D.

Let

$$u(x, y) = \sum_{j=1}^{n} c_j \phi_j(x, y) \tag{5}$$

where n is number of vertices.

Let m be the number of internal vertices. The other vertices are the ones on the boundary of D. We pick the constants c_j so that

$$\frac{\partial I}{\partial c_j} = 0 \quad \text{for } 1 \leq j \leq m.$$

From the expression of I in equation (1), we apply the chain rule to obtain

$$0 = \iint_D \left[2\frac{\partial u}{\partial x}\frac{\partial u_x}{\partial c_j} + 2\frac{\partial u}{\partial y}\frac{\partial u_y}{\partial c_j} \right] dA \tag{6}$$

for $1 \leq j \leq m$. In equation (4), u_x and u_y are the partial derivatives of u with respect to the variables x and y. This equation is a condition for each index j, and so there are m conditions in total. Now,

$$\frac{\partial u}{\partial x} = \sum_{j=1}^{n} c_j \frac{\partial}{\partial x} \phi_j(x, y) \tag{7}$$

and since $\frac{\partial u}{\partial c_j} = \phi_j(x, y)$, we also have

$$\frac{\partial u_x}{\partial c_j} = \frac{\partial \phi_j}{\partial x} \tag{8}$$

Substitute equation (7) into (4) to obtain

$$0 = \iint_D \left[2 \frac{\partial u}{\partial x} \frac{\partial \phi_j}{\partial x} + 2 \frac{\partial u}{\partial y} \frac{\partial \phi_j}{\partial y} \right] dA; \;\; for\, 1 \leq j \leq m. \tag{9}$$

Divide the domain D into p triangles $\{T_i\}_{i=1}^{p}$ and the last equation becomes

$$0 = 2 \sum_{i=1}^{p} \iint_{T_i} \left[\frac{\partial u}{\partial x} \frac{\partial \phi_j}{\partial x} + \frac{\partial u}{\partial y} \frac{\partial \phi_j}{\partial y} \right] dA; \;\; for\, 1 \leq j \leq m. \tag{10}$$

The function $\phi_j(x, y)$ is linear on triangle T_i and we write ϕ_{ij} to denote the restriction of ϕ_j to triangle T_i so that

$$\phi_{ij}(x, y) = a_{ij}x + b_{ij}y + d_{ij}$$

where a_{ij} , b_{ij} and d_{ij} are constants. These constants associated with each triangle for ϕ_j are uniquely determined by the three vertices of the triangle. From the last equation, we see that

$$\frac{\partial \phi_{ij}}{\partial x} = a_{ij} \quad and \quad \frac{\partial \phi_{ij}}{\partial y} = b_{ij} \tag{11 \& 12}$$

Note that

$$\frac{\partial u}{\partial x} = \sum_{k=1}^{n} c_k a_{ik} \tag{13}$$

and

$$\frac{\partial u}{\partial y} = \sum_{k=1}^{n} c_k b_{ik} \tag{14}$$

Therefore, equation (8) becomes

$$0 = 2 \sum_{i=1}^{p} \iint_{T_i} \left[\left(\sum_{k=1}^{n} c_k a_{ik} \right) a_{ij} + \left(\sum_{k=1}^{n} c_k b_{ik} \right) b_{ij} \right] dA; \;\; for\, 1 \leq j \leq m. \tag{15}$$

Note that the quantity in each bracket is a constant on triangle T_i . Let A_i be the area of triangle T_i. Then, for $1 \leq j \leq m$,

$$0 = \sum_{i=1}^{p} \left[\left(\sum_{k=1}^{n} c_k a_{ik} \right) a_{ij} + \left(\sum_{k=1}^{n} c_k b_{ik} \right) b_{ij} \right] A_i \tag{16}$$

If we interchange the sums, then we can write the last expression as

$$0 = \sum_{k=1}^{n} c_k \left(\sum_{i=1}^{p} [a_{ik}\, a_{ij} + b_{ik}\, b_{ij}]\ A_i \right) \tag{17}$$

which is a condition for each j, where $1 \leq j \leq m$. For each j, there is one equation with n variables c_k. But only m of the c_k are unknown. The remaining vertices are ones on the boundary of D. For any vertex on the boundary of D, we set c_J to be the value of $z(x, y)$ on that vertex. That means, we have a system of m equations in m unknown variables, and so we can solve for c_k.

Atlantis Triangulation

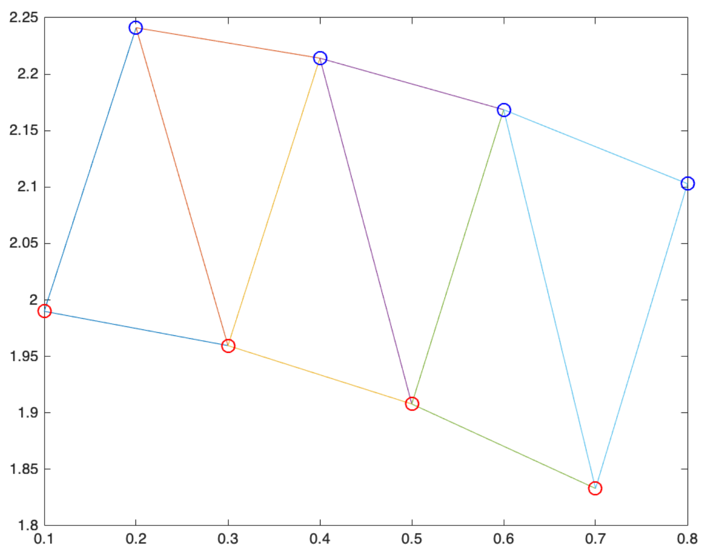

Figure 14. Triangles between two sets of vertices

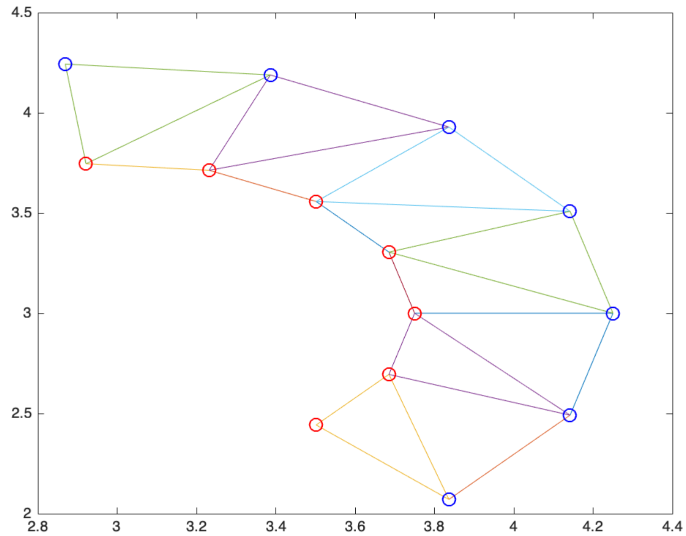

Figure 15. Atlantis triangulation using 14 vertices

Suppose we want to divide a domain into triangles. The outer boundary is one curve. The inner boundary is another curve. We can draw curves between these two boundaries. Places vertices on these curves. To start the procedure, begin with any two adjacent curves, connect the vertices from one curve to the vertices on the other curve, and continue in this manner, using a sawtooth pattern (i.e. zig-pattern) to draw triangles. Figure 14 shows the triangulation of a domain by drawing sawtooth wave (i.e. zig-zag pattern) between the two sets of vertices. For clarity, we illustrate with red vertices on one curve and blue vertices on the other curve. For comparison, Figure 15 and Figure 16 shows the construction by Atlantis and Delaunay triangulation, respectively, for the same set of 14 vertices.

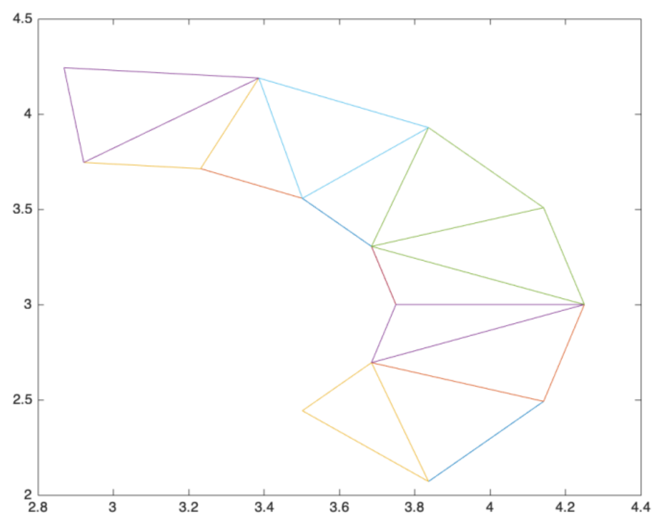

Figure 16. Delaunay triangulation using 14 vertices